

# Weak Decays of Doubly Heavy Baryons: $\mathcal{B}_{cc} \rightarrow \mathcal{B}D^{(*)}$

Run-Hui Li\*, Juan-Juan Hou, Bei He, Ya-Ru Wang

*School of Physical Science and Technology, Inner Mongolia University, Hohhot 010021, China*

The discovery of  $\Xi_{cc}^{++}$  inspires the new interest in studying the doubly heavy baryons. In this paper the weak decays of a doubly charm baryons  $\mathcal{B}_{cc}$  to a light baryon  $\mathcal{B}$  and a charm meson  $D^{(*)}$  (either a pseudoscalar or a vector one) are calculated. Following our previous work, we calculate the short distance contributions under the factorization hypothesis and the long distance contributions are modeled as the final state interactions which are calculated with the one particle exchange model. We find that the  $\mathcal{B}_{cc} \rightarrow \mathcal{B}D^*$  decays' branching ratios are obviously larger, since they receive contributions from more polarization states. Among the decays we investigated, the following ones have the largest branching fractions.  $\mathcal{BR}(\Xi_{cc}^{++} \rightarrow \Sigma^+ D^{*+}) \in [0.46\%, 3.33\%]$  estimated with  $\tau_{\Xi_{cc}^{++}} = 256$  fs,  $\mathcal{BR}(\Xi_{cc}^+ \rightarrow \Lambda D^{*+}) \in [0.38\%, 2.63\%]$  and  $\mathcal{BR}(\Xi_{cc}^+ \rightarrow \Sigma^0 D^{*+}) \in [0.45\%, 3.16\%]$  with  $\tau_{\Xi_{cc}^+} = 45$  fs,  $\mathcal{BR}(\Omega_{cc}^+ \rightarrow \Xi^0 D^{*+}) \in [0.27\%, 1.03\%]$ ,  $\mathcal{BR}(\Omega_{cc}^+ \rightarrow \Xi^0 D^+)$   $\in [0.07\%, 0.44\%]$  and  $\mathcal{BR}(\Omega_{cc}^+ \rightarrow \Sigma^0 D^{*+}) \in [0.06\%, 0.45\%]$  with  $\tau_{\Omega_{cc}^+} = 75$  fs. Topologically, all  $\mathcal{B}_{cc} \rightarrow \mathcal{B}D^{(*)}$  processes are pure bow tie diagram decays. The fact that some branching fractions of these decays can reach percentage level indicates that the bow tie topology may also play an important role at the charm scale.

PACS numbers: 13.30.-a, 12.40.-y, 12.15.-y, 12.39.Fe

## I. INTRODUCTION

The study on doubly heavy baryons which contain two heavy constituent quarks ( $c$  or  $b$  quark) has lasted for a long time. They are predicted by the quark model and allowed by the quantum chromodynamics theory. Physicists believe their existence, even though they had not appeared in experiments. The SELEX collaboration used to announce the discovery of  $\Xi_{cc}^+$  in 2002 and 2005[1, 2]. However, they reported quite large production and long life time for this particle which is different a lot from theoretical predictions and is not confirmed by the other experiments. In 2017 the LHCb collaboration declared the discovery of  $\Xi_{cc}^{++}$  via  $\Xi_{cc}^{++} \rightarrow \Lambda_c^+ K^- \pi^+ \pi^+$  with a mass as 3.621 GeV[3]. In 2018 the LHCb collaboration measure its lifetime as 256 fs[4] and confirmed their discovery via  $\Xi_{cc}^{++} \rightarrow \Xi_c^+ \pi^+$ [5].  $\Xi_{cc}^{++}$  is the first doubly heavy baryon discovered in experiments that owns theoretically expected properties. Its discovery is meaningful to the study of hadron spectrum and baryon decays. Physicists have already done a lot of research on the spectrum of doubly heavy baryons. However, figuring out a proper frame work for their weak decays is a really challenging task. A lot of studies on this topic has been performed [6–18], and form factors as well as the semileptonic decays of a doubly heavy baryon to a singly heavy baryon are studied under various of frameworks. However, there is still not any systematic method to deal with even the two body nonleptonic decays, which is essential to guide new particle discoveries, understand the dynamics of strong interaction, and test the standard model precisely.

In 2017 we applied the final state interactions (FSIs) to baryon decays at the charm scale to realize the calculation of two body nonleptonic weak decays of doubly charm baryons [19]. We presented two golden discovery channels for  $\Xi_{cc}^{++}$  under this framework, which, mentioned above, are adopted by the LHCb collaboration and help to discover the  $\Xi_{cc}^{++}$  particle. The discovery inspires the research on doubly heavy baryons and more questions are presented. Which are the golden discovery channels for the other doubly charm baryons and what can we find in the decays of doubly charm baryons? To answer these questions, more research on the weak decays of doubly heavy baryons are required. In our previous work, we calculate the decays of a doubly charm baryon to a singly charm baryon and a light vector meson as well as explore those decays for some potential discovery channels [20]. After discovering  $\Xi_{cc}^{++}$ , measuring its lifetime, and confirming the discovery with another decay, the LHCb collaboration also pay attention to the weak decays of  $\Xi_{cc}^{++}$  with a charm meson in the final state [21]. Motivated by the theoretical questions and experimental efforts, we study the two body nonleptonic decays of a doubly charm baryon  $\mathcal{B}_{cc} \rightarrow \mathcal{B}D^{(*)}$  in this paper, where  $\mathcal{B}_{cc}$  represents a doubly charm baryon,  $\mathcal{B}$  denotes a light baryon, and  $D^{(*)}$  is either a pseudoscalar or a vector charm meson.

There are many interesting physics to be explored in baryon decays. For example, the  $CP$  violations have already been observed in  $K$ ,  $B$  and  $D$  meson decays, but not been observed in baryon decays. Theoretical development on this topic is slow because calculations of the dynamics is a challenging work. No systematic factorization method

---

\* E-mail: lirh@imu.edu.cn

is established so far even for the two body nonleptonic decays. Usually the contributions in two body nonleptonic baryon decays are usually classified topologically into several types as  $T$  (W external emission),  $C$  (color suppressed),  $E$  (W exchange) and  $B$  (bow tie). In  $b$  baryon decays the  $E$  and  $B$  contributions are numerically small[22]. In the charm sector the picture may be quite different and the  $E$  and  $B$  contributions may become important. The decays investigated in this paper are purely  $B$  type ones, the study on which will help to understand the dynamics of baryon decays at the charm scale.

This paper is organized as follows. In section II the contributions and the phenomenological framework is introduced. In section III we collect values of some inputs, tables of our results and present our discussions. In section IV a summary is given. For shortage of the paper, we list all the expressions for the amplitudes in appendix A and the strong couplings are gathered in appendix B.

## II. THEORETICAL FRAMEWORK AND ANALYTICAL CALCULATIONS

### A. On the Framework

In our previous work we extend the model of final state interactions to baryon decays [19, 20] and suggest the discovery channels for  $\Xi_{cc}^{++}$  successfully. In our work we also find a misunderstanding on FSIs in some earlier literatures, and interested readers are referred to our upcoming paper. In the start of this section we would like introduce this framework briefly by following the ideas proposed in the Ref. [28]. Supposed the weak Hamiltonian is in the form  $\mathcal{H}_W = \lambda_i Q_i$  with  $\lambda_i$  representing the combinations of quark mixing matrix elements and  $Q_i$  are time reversal invariant weak operators, the amplitude of  $\mathcal{B}_{cc} \rightarrow i$  can be decomposed as

$$\langle i; \text{out} | Q | \mathcal{B}_{cc}; \text{in} \rangle^* = \sum_j S_{ji}^* \langle j; \text{out} | Q | \mathcal{B}_{cc}; \text{in} \rangle, \quad (1)$$

where  $S_{ji} \equiv \langle i; \text{out} | j; \text{in} \rangle$  is the strong interaction  $S$  matrix element. Using the unitarity of the  $S$ -matrix and  $S = 1 + iT$ , one can obtain a identity related to the optical theorem as

$$2\text{Abs} \langle i; \text{out} | Q | \mathcal{B}_{cc}; \text{in} \rangle = \sum_j T_{ji}^* \langle j; \text{out} | Q | \mathcal{B}_{cc}; \text{in} \rangle. \quad (2)$$

Specifically, for  $\mathcal{B}_{cc} \rightarrow \mathcal{B}D^{(*)}$  decay, the absorptive part of the amplitude can be obtained as

$$\begin{aligned} \text{Abs} \mathcal{M}(\mathcal{B}_{cc} \rightarrow \mathcal{B}D^{(*)}) &= \frac{1}{2} \sum_j \left( \prod_{k=1}^j \int \frac{d^3 q_k}{(2\pi)^3 2E_k} \right) (2\pi)^4 \delta^4(p_{\mathcal{B}} + p_{D^{(*)}} - \sum_{k=1}^j q_k) \\ &\times \mathcal{M}(p_{\mathcal{B}_{cc}} \rightarrow \{q_k\}) T^*(p_{\mathcal{B}} p_{D^{(*)}} \rightarrow \{q_k\}). \end{aligned} \quad (3)$$

Eq.(1) and (3) indicate that the decay process is modeled as two steps. One is the generation of an intermediate state under weak interactions, which is dominated by short distance dynamics, the other is the formation of a final state subsequently through the strong interactions among intermediate particles. In principle one have to consider all the possible intermediate states. However, basing on the argument that the 2-body  $\rightleftharpoons$   $n$ -body rescattering is negligible [23] we only need consider the intermediate states with two particles.

The weak decays  $\mathcal{B}_{cc} \rightarrow \mathcal{B}D^{(*)}$  are induced by charged current  $c \rightarrow s/d$ . For charm decays induced by the flavor changing neutral current with quark loop effect, there exists cancellation between  $d$  and  $s$  quark loop contributions, therefore the FCNC contributions can be ignored safely. The low energy effective hamiltonian with charged current is given by

$$\mathcal{H}_{eff} = \frac{G_F}{\sqrt{2}} \sum_{q=d,s} V_{cq}^* V_{uq} [C_1(\mu) O_1^q(\mu) + C_2(\mu) O_2^q(\mu)] + \text{h.c.}, \quad (4)$$

with

$$O_1^q = (\bar{u}_\alpha D_\beta)_{V-A} (\bar{q}_\beta c_\alpha)_{V-A}, \quad O_2^q = (\bar{u}_\alpha D_\alpha)_{V-A} (\bar{q}_\beta c_\beta)_{V-A}, \quad (5)$$

where  $D = s, d$ ,  $V_{cq}$  and  $V_{uq}$  are the Cabibbo-Kobayashi-Maskawa (CKM) matrix elements whose values are used from the CKMfitter Group [24],  $C_{1/2}(\mu)$  stand for the Wilson coefficients, the Fermi constant  $G_F = 1.166 \times 10^{-5} \text{ GeV}^{-2}$ , and  $O_{1/2}^q$  are the local four-quark operators in which  $\alpha$  and  $\beta$  are color indices.

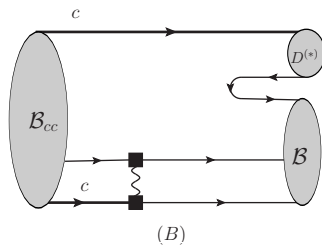


FIG. 1: Bow-tie diagram. It is kind of  $W$  exchange mechanism with weakly generating quarks taken all by the final state baryon

The contributions induced by the above Hamiltonian in two body nonleptonic  $\mathcal{B}_{cc}$  can be classified into eight topological diagrams, and readers are referred to Ref. [20] for details. In the bow-tie diagram, depicted in the Fig. 1, the quarks generated at weak vertex are all absorbed by the final state baryon. Here this diagram only show the topological structure of weak interactions. The strong interactions, both short and long distance, are all included although they are not drawn. As stated in the introduction part, the decays considered in this paper are all pure bow-tie contribution, which is type of  $W$  exchange contribution. The study on these decays can help to figure out the role of  $W$ -exchange contribution in charm decays, and furthermore help to promote the study on charm meson decays.

A final state  $\mathcal{B}D^{(*)}$  may be generated either directly at short distance or at long distance via interactions among some short-distance-generated intermediate states. In  $\mathcal{B}_{cc} \rightarrow \mathcal{B}D^{(*)}$  decays the short-distance-direct-production mechanism belongs to the  $B$  topological diagram, which is thought to be much smaller than the  $T$  contribution. What's more, In charm decays the long distance contribution is thought to be dominating because of low energy release [25]. Therefore, in this paper the direct-generation dynamics at short distance is neglected and the long distance production through interactions among intermediate particles is taken into consideration. For a rough estimation considering those long distance contributions with  $T$  or  $C$  weak dynamics are enough. Basing on these arguments, the calculation of  $\mathcal{B}_{cc} \rightarrow \mathcal{B}D^{(*)}$  is realized by  $\mathcal{B}_{cc} \rightarrow \mathcal{B}_c\mathcal{M} \rightarrow \mathcal{B}D^{(*)}$ , where  $\mathcal{B}_c$  is a singly charm baryon and  $\mathcal{M}$  is a light meson. The long distance part  $\mathcal{B}_c\mathcal{M} \rightarrow \mathcal{B}D^{(*)}$ , nonperturbative essentially, is hard to be calculated. In this work we model it as the final state interactions (FSIs) and perform the calculation at hadron level. In this model, the long distance dynamics are realized by exchanging hadron-state particles (depicted in Fig. 2). Now we arrive at the stage to calculate an amplitude in details.

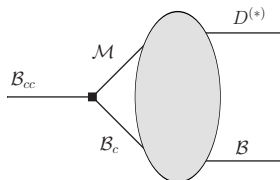


FIG. 2: Decay process indicated at hadron level. The black square is a weak vertex at which the intermediate state  $\mathcal{B}_c\mathcal{M}$  is generated. The gray ellipse represents the strong interactions between intermediate particles, which is realized by exchanging hadron states

## B. Calculation of weak vertices

As stated in the above subsection, the first step to get an amplitude is to calculate the weak production of an intermediate state under  $T$  or  $C$  mechanism. At hadron level this part is represented by a weak vertex. Since it is  $T$  or  $C$  mechanism, the weak vertex can be calculated reliably with the factorization hypothesis. Given the Hamiltonian in Eqs. (4) and (5), a  $T$  diagram in the factorization hypothesis is factorized as

$$\mathcal{A}(\mathcal{B}_{cc} \rightarrow \mathcal{B}_c\mathcal{M}) = \frac{G_F}{\sqrt{2}} \sum_{q=d,s} V_{cq}^* V_{uq} (C_2 + C_1/N_C) \langle \mathcal{M} | (\bar{u}_\alpha D_\alpha)_{V-A} | 0 \rangle \langle \mathcal{B}_c | (\bar{q}_\beta c_\beta)_{V-A} | \mathcal{B}_{cc} \rangle. \quad (6)$$

The weak transition of  $\mathcal{B}_{cc}$  to a spin-1/2 singly charm baryon  $\mathcal{B}_c$  is parameterized as

$$\begin{aligned} \langle \mathcal{B}_c(p', s'_z) | (V - A)_\mu | \mathcal{B}_{cc}(p, s_z) \rangle = & \bar{u}(p', s'_z) \left[ \gamma_\mu f_1(q^2) + i\sigma_{\mu\nu} \frac{q^\nu}{M} f_2(q^2) + \frac{q^\mu}{M} f_3(q^2) \right] u(p, s_z) \\ & - \bar{u}(p', s'_z) \left[ \gamma_\mu g_1(q^2) + i\sigma_{\mu\nu} \frac{q^\nu}{M} g_2(q^2) + \frac{q^\mu}{M} g_3(q^2) \right] \gamma_5 u(p, s_z), \end{aligned} \quad (7)$$

with  $q = p - p'$ ,  $M$  is the mass of  $\mathcal{B}_{cc}$  and  $f_i, g_i$  are the form factors.

The expressions of  $f_i$  and  $g_i$ , which can be obtained with the help of kinds of quark models or sum rules, are used as inputs here. In this paper we adopt the results calculated under the light-front quark model in Refs. [10, 26].

The decay constants of pseudoscalar and vector mesons are defined with axial-vector current and vector current, respectively.

$$\langle 0 | A_\mu | P(q) \rangle = i f_P q_\mu, \quad (8)$$

and

$$\langle 0 | V_\mu | V(q) \rangle = f_V m_V \epsilon_\mu, \quad (9)$$

where the “ $P$ ” and “ $V$ ” in subscripts correspond to a pseudoscalar and vector meson, respectively. Combining Eqs. (7), (8) and (9), we present the weak vertex of  $\mathcal{B}_{cc} \rightarrow \mathcal{B}_c P$  as

$$W_T(\mathcal{B}_{cc} \rightarrow \mathcal{B}_c P) = i \frac{G_F}{\sqrt{2}} V_{cq}^* V_{uD} a_1 f_P \bar{u}(p', s'_z) \left[ (M - M') f_1(m_P^2) + (M + M') g_1(m_P^2) \gamma_5 \right] u(p, s_z). \quad (10)$$

$C$  diagram can be calculated via its relation to  $T$  diagram under Fierz transformation,

$$W_C(\mathcal{B}_{cc} \rightarrow \mathcal{B}_c P) = i \frac{G_F}{\sqrt{2}} V_{cq}^* V_{uD} a_2 f_P \bar{u}(p', s'_z) \left[ (M - M') f_1(m_P^2) + (M + M') g_1(m_P^2) \gamma_5 \right] u(p, s_z). \quad (11)$$

In the above equations  $a_1 = C_2 + C_1/N_C$  and  $a_2 = C_1 + C_2/N_C$  are the combinations of Wilson coefficients. In this work, the decays are under the charm scale, so we use  $a_1(m_c)$  and  $a_2(m_c)$  in Ref. [27].  $M'$  is the mass of  $\mathcal{B}_c$ . We omit the terms with  $f_3$  and  $g_3$  in Eq. (11), for they are suppressed by  $m_P^2/M^2$ .

For  $\mathcal{B}_{cc} \rightarrow \mathcal{B}_c V$  there are

$$\begin{aligned} W_T(\mathcal{B}_{cc} \rightarrow \mathcal{B}_c V) = & \frac{G_F}{\sqrt{2}} V_{cq}^* V_{uD} a_1 f_V \epsilon_\mu^* \bar{u}(p', s'_z) \left[ \left( f_1(m_V^2) - \frac{M + M'}{M} f_2(m_V^2) \right) \gamma^\mu + \frac{2}{M} f_2(m_V^2) p'^\mu \right. \\ & \left. - \left( g_1(m_V^2) + \frac{M - M'}{M} g_2(m_V^2) \right) \gamma^\mu \gamma_5 - \frac{2}{M} g_2(m_V^2) p'^\mu \gamma_5 \right] u(p, s_z), \\ W_C(\mathcal{B}_{cc} \rightarrow \mathcal{B}_c V) = & \frac{G_F}{\sqrt{2}} V_{cq}^* V_{uD} a_2 f_V \epsilon_\mu^* \bar{u}(p', s'_z) \left[ \left( f_1(m_V^2) - \frac{M + M'}{M} f_2(m_V^2) \right) \gamma^\mu + \frac{2}{M} f_2(m_V^2) p'^\mu \right. \\ & \left. - \left( g_1(m_V^2) + \frac{M - M'}{M} g_2(m_V^2) \right) \gamma^\mu \gamma_5 - \frac{2}{M} g_2(m_V^2) p'^\mu \gamma_5 \right] u(p, s_z). \end{aligned} \quad (12)$$

### C. Rescattering at long distance

The rescattering between the intermediate particles is nonperturbative dynamics in nature and really difficult to calculate. In this work we employ the framework of FSIs and perform the calculation with one-particle-exchange model at the hadron level [25, 28, 29]. In the following, we take  $\Omega_{cc}^+ \rightarrow \Xi^0 D_s^+$  as an example to show the detailed progress of our calculation. This decay can proceed as  $\Omega_{cc}^+ \rightarrow \Omega_c^0(K^+/K^{*+}) \rightarrow \Xi^0 D_s^+$ ,  $\Omega_{cc}^+ \rightarrow (\Xi_c^+/\Xi_c'^+)(\phi/\eta_1/\eta_8) \rightarrow \Xi^0 D_s^+$  and  $\Omega_{cc}^+ \rightarrow (\Xi_c^0/\Xi_c'^0)(\pi^+/\rho^+) \rightarrow \Xi^0 D_s^+$ . The first one is induced by  $c \rightarrow s u \bar{s}$  at quark level and the last two ones are induced by  $c \rightarrow d u \bar{d}$ , which indicates it a singly CKM suppressed decay. The intermediate states  $\Omega_c^0(K^+/K^{*+})$  and  $(\Xi_c^0/\Xi_c'^0)(\pi^+/\rho^+)$  are generated via the  $T$  diagram and  $(\Xi_c^+/\Xi_c'^+)(\phi/\eta_1/\eta_8)$  origin from  $C$  mechanism.

As mentioned above and depicted in Fig. 2, the long distant contributions are calculated at hadron level. The calculation is performed with the help of the chiral Lagrangian. One can draw all the leading diagrams in the meaning of perturbation theory with only one particle exchanged as in Fig. 3. The Lagrangian used in this paper are from Refs. [30–33]. The readers can refer to Ref. [19] for specific expressions.

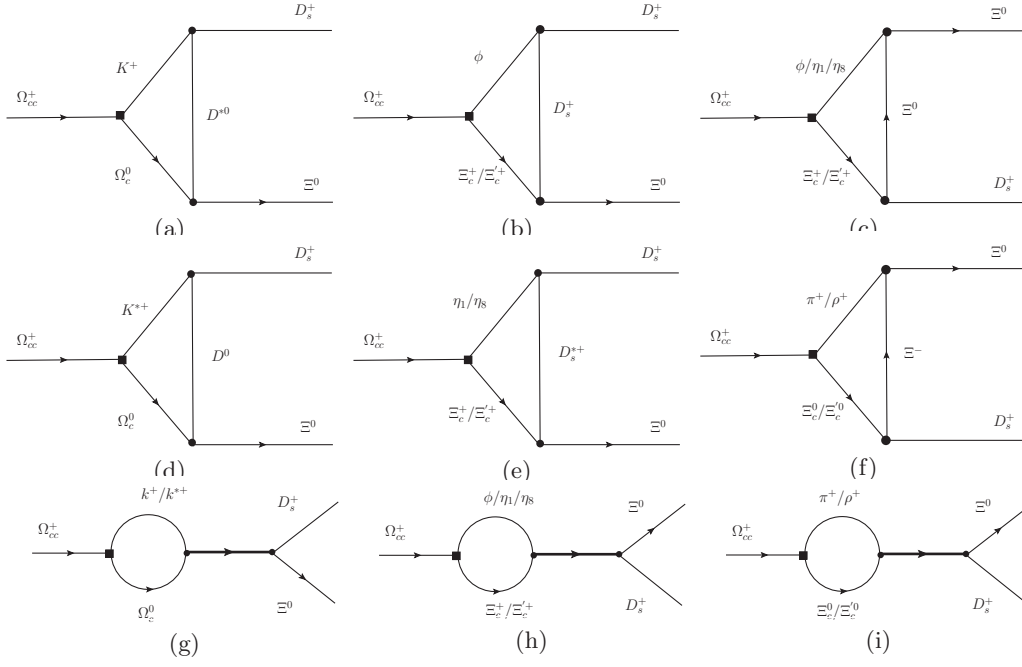


FIG. 3: Leading FSI contributions to  $\Omega_{cc}^+ \rightarrow \Xi^0 D_s^+$  manifested at hadron level. The black squares denote weak vertices and dots represent strong vertices. Each thick line in diagram (g), (h) and (i) denotes a resonant structure. Diagrams (a), (d) and (g) are induced by the rescattering between  $\Omega_c^0$  and  $K^+/K^{*+}$ , diagrams (b), (c), (e) and (h) by the rescattering between  $\Xi_c^+/\Xi_c'^+$  and  $\phi/\eta_1/\eta_8$ , and diagram (f) by  $\Xi_c^0/\Xi_c'^0$  and  $\pi^+/\rho^+$

The three diagrams of  $s$  channel, Figs. 3(g), (h) and (i), contributes sizably only when the mass of each resonant state is quite near to that of the mother particle  $\Omega_{cc}^+$ . Among the discovered singly charmed baryons even the heaviest one is about 500 MeV lighter than  $\Xi_{cc}^{++}$ . Therefore, these contributions are supposed to be suppressed by the off-shell effect. As a result we neglect these contributions in our calculation and only consider the  $t$  channel contributions which are typical triangle diagrams depicted in Figs. 3(a)-(f). Eq. (3) is employed to calculate the absorptive part of these diagrams. In principle the dispersive part can be obtained via the dispersion relation

$$\text{Dis } A(m_1^2) = \frac{1}{\pi} \int_s^\infty \frac{\text{Abs } A(s')}{s' - m_1^2} ds', \quad (13)$$

which is hard to be calculated and leads to a large ambiguity [28]. We follow the scheme adopted in Ref. [28] and set absorptive part as dominating and ignore the dispersive one. In addition a structure named form factor is associated with the exchanged particle to account for its off-shell effect and make the theoretical model self-consistent. More details are talked about in the next subsection.

#### D. Analytic expressions for the diagrams

Combing the discussions in section II B and II C, we derive the analytic expressions for the amplitudes in this subsection. In order to simplify the subscripts we assign some numbers to the particles in a triangle diagram as shown in Fig. 4, in which the momentum flows are also defined. We use  $M_{a/b/c/d/e/f}(P2; P3; P4)$  to denote the amplitude of such a triangle diagram. The subscripts “ $a/b/c/d/e/f$ ” correspond to Figs. 3(a)-(f), and  $P2$ ,  $P3$  and  $P4$  denote the particles at positions 2, 3 and 4, respectively.

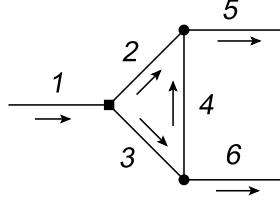


FIG. 4: Numbers assigned to the lines in a triangle diagram. The arrows define the momentum directions in our calculation

Specificly, the absorptive part of Fig. 3(a) is given by set  $P2 = K^+$ ,  $P3 = \Omega_c^0$  and  $P4 = D^{*0}$

$$\begin{aligned}
Abs M_a(K^+; \Omega_c^0; D^{*0}) &= \int \frac{|\vec{p}_2| \sin\theta d\theta d\varphi}{32\pi^2 m_{\Omega_{cc}^+}} \frac{G_F}{\sqrt{2}} V_{cs}^* V_{us} a_1 f_{K^+} \frac{F^2(t, m_{D^{*0}})}{t - m_{D^{*0}}^2 + im_{D^{*0}} \Gamma_{D^{*0}}} g_{D^{*0} D_s^+ K^+ P2\alpha} \\
&\times \bar{u}(p_6, s'_z) \left[ f_{1\Omega_c^0 \Xi^0 D^{*0}} \gamma_\mu \left( -g^{\mu\alpha} + \frac{p_4^\mu p_4^\alpha}{m_{D^{*0}}^2} \right) + \frac{f_{2\Omega_c^0 \Xi^0 D^{*0}}}{m_{\Omega_c^0} + m_{\Xi^0}} \sigma_{\mu\nu} i p_4^\mu \left( -g^{\nu\alpha} + \frac{p_4^\nu p_4^\alpha}{m_{D^{*0}}^2} \right) \right] \\
&\times (\not{p}_3 + m_{\Omega_c^0}) \left[ (m_{\Omega_{cc}^+} - m_{\Omega_c^0}) f_1(m_{K^+}^2) + (m_{\Omega_{cc}^+} + m_{\Omega_c^0}) g_1(m_{K^+}^2) \gamma_5 \right] u(p_1, s_z). \quad (14)
\end{aligned}$$

In calculation summations over the polarization states of intermediate and exchanged particles, i.e.  $\Omega_c^0$  and  $D^{*0}$  in Fig. 3(a) since  $K^+$  is a pseudoscalar meson, need to be performed.  $\theta$  and  $\phi$  in Eq. (14) are the polar and azimuthal angles of  $\vec{p}_3$  in spherical coordinate system.  $g_{D^{*0} D_s^+ K^+}$ ,  $f_{1\Omega_c^0 \Xi^0 D^{*0}}$  and  $f_{2\Omega_c^0 \Xi^0 D^{*0}}$  are strong coupling constants.  $P2$  and  $P3$  are set to be on-shell. To account for the off-shell effect and make the theoretical framework self-consistent, a Breit-Wigner structure and a form factor  $F(t, m)$  are associated with the exchanged particle. The form factor  $F(t, m)$  is parameterized as [28]

$$F(t, m) = \left( \frac{\Lambda^2 - m^2}{\Lambda^2 - t} \right)^n, \quad (15)$$

normalized to 1 at  $t = m^2$ .  $m$  is the mass of the exchanged particle. The cutoff  $\Lambda$  is given as

$$\Lambda = m + \eta \Lambda_{\text{QCD}} \quad (16)$$

with  $\Lambda_{\text{QCD}} = 330$  MeV. The phenomenological parameter  $\eta$  depends on all the particles at the strong vertex. Because a large number of strong vertices appear in the calculation, one requires huge amount of experimental data to determine these parameters one by one. In our calculation we simply set  $\eta = 1.5$  and vary it from 1 to 2 for error estimations.  $n$  in Eq. (15) is another phenomenological parameter that needs to be extracted from experimental data. For lack of experimental data, we borrow the experience from Ref. [28] and set it to 1.

Similarly for Fig. 3(d), there is

$$\begin{aligned}
Abs M_d(K^{*+}; \Omega_c^0; D^0) &= -i \int \frac{|\vec{p}_2| \sin\theta d\theta d\varphi}{32\pi^2 m_{\Omega_{cc}^+}} \frac{G_F}{\sqrt{2}} V_{cs}^* V_{us} a_1 f_{K^{*+}} \frac{F^2(t, m_{D^0})}{t - m_{D^0}^2 + im_{D^0} \Gamma_{D^0}} g_{\Omega_c^0 \Xi^0 D^0} g_{D_s^+ D^0 K^{*+}} (p_{5\alpha} + p_{4\alpha}) \\
&\times \bar{u}(p_6, s'_z) \gamma_5 (\not{p}_3 + m_{\Omega_c^0}) \left( -g^{\mu\alpha} + \frac{p_2^\mu p_2^\alpha}{m_{K^{*+}}^2} \right) \\
&\times \left[ \left( f_1(m_{K^{*+}}^2) - \frac{m_{\Omega_{cc}^+} + m_{\Omega_c^0}}{m_{\Omega_{cc}^+}} f_2(m_{K^{*+}}^2) \right) \gamma_\mu + \frac{2}{m_{\Omega_{cc}^+}} f_2(m_{K^{*+}}^2) p_{3\mu} \right. \\
&\left. - \left( g_1(m_{K^{*+}}^2) + \frac{m_{\Omega_{cc}^+} - m_{\Omega_c^0}}{m_{\Omega_{cc}^+}} g_2(m_{K^{*+}}^2) \right) \gamma_\mu \gamma_5 - \frac{2}{m_{\Omega_{cc}^+}} g_2(m_{K^{*+}}^2) p_{3\mu} \gamma_5 \right] u(p_1, s_z), \quad (17)
\end{aligned}$$

where the spin summation over the polarization states of  $\Omega_c^0$  and  $K^{*+}$  is performed. It should be stressed that some symbols of strong coupling constants looks similar to those of weak transition form factors, and one can distinguish them by the feature that strong coupling constants have particle names as subscripts. The expressions for the rest

diagrams in Fig. 3 are given as follows.

$$\begin{aligned}
Abs M_b(\phi; \Xi_c^+; D_s^+) &= i \int \frac{|\vec{p}_2| \sin\theta d\theta d\varphi}{32\pi^2 m_{\Omega_{cc}^+}} \frac{G_F}{\sqrt{2}} V_{cs}^* V_{us} a_2 f_\phi \frac{F^2(t, m_{D_s^+})}{t - m_{D_s^+}^2 + im_{D_s^+} \Gamma_{D_s^+}} g_{\Xi_c^+ \Xi^0 D_s^+} g_{D_s^+ D_s^+ \phi} (p_{4\alpha} + p_{5\alpha}) \\
&\times \bar{u}(p_6, s'_z) \gamma_5 (\not{p}_3 + m_{\Xi_c^+}) (-g^{\mu\alpha} + \frac{p_2^\mu p_2^\alpha}{m_\phi^2}) \\
&\times \left[ \left( f_1(m_\phi^2) - \frac{m_{\Omega_{cc}^+} + m_{\Xi_c^+}}{m_{\Omega_{cc}^+}} f_2(m_\phi^2) \right) \gamma_\mu + \frac{2}{m_{\Omega_{cc}^+}} f_2(m_\phi^2) p_{3\mu} \right. \\
&\left. - \left( g_1(m_\phi^2) + \frac{m_{\Omega_{cc}^+} - m_{\Xi_c^+}}{m_{\Omega_{cc}^+}} g_2(m_\phi^2) \right) \gamma_\mu \gamma_5 - \frac{2}{m_{\Omega_{cc}^+}} g_2(m_\phi^2) p_{3\mu} \gamma_5 \right] u(p_1, s_z). \tag{18}
\end{aligned}$$

$$\begin{aligned}
Abs M_b(\phi; \Xi_c'^+; D_s^+) &= i \int \frac{|\vec{p}_2| \sin\theta d\theta d\varphi}{32\pi^2 m_{\Omega_{cc}^+}} \frac{G_F}{\sqrt{2}} V_{cs}^* V_{us} a_2 f_\phi \frac{F^2(t, m_{D_s^+})}{t - m_{D_s^+}^2 + im_{D_s^+} \Gamma_{D_s^+}} g_{\Xi_c'^+ \Xi^0 D_s^+} g_{D_s^+ D_s^+ \phi} (p_{4\alpha} + p_{5\alpha}) \\
&\times \bar{u}(p_6, s'_z) \gamma_5 (\not{p}_3 + m_{\Xi_c'^+}) (-g^{\mu\alpha} + \frac{p_2^\mu p_2^\alpha}{m_\phi^2}) \\
&\times \left[ \left( f_1(m_\phi^2) - \frac{m_{\Omega_{cc}^+} + m_{\Xi_c'^+}}{m_{\Omega_{cc}^+}} f_2(m_\phi^2) \right) \gamma_\mu + \frac{2}{m_{\Omega_{cc}^+}} f_2(m_\phi^2) p_{3\mu} \right. \\
&\left. - \left( g_1(m_\phi^2) + \frac{m_{\Omega_{cc}^+} - m_{\Xi_c'^+}}{m_{\Omega_{cc}^+}} g_2(m_\phi^2) \right) \gamma_\mu \gamma_5 - \frac{2}{m_{\Omega_{cc}^+}} g_2(m_\phi^2) p_{3\mu} \gamma_5 \right] u(p_1, s_z). \tag{19}
\end{aligned}$$

$$\begin{aligned}
Abs M_e(\eta_1; \Xi_c^+; D_s^{*+}) &= - \int \frac{|\vec{p}_2| \sin\theta d\theta d\varphi}{32\pi^2 m_{\Omega_{cc}^+}} \frac{G_F}{\sqrt{2}} V_{cs}^* V_{us} a_2 f_{\eta_1} \frac{F^2(t, m_{D_s^{*+}})}{t - m_{D_s^{*+}}^2 + im_{D_s^{*+}} \Gamma_{D_s^{*+}}} g_{D_s^{*+} D_s^+ \eta_1} p_{2\alpha} \\
&\times \bar{u}(p_6, s'_z) \left[ f_{1\Xi_c^+ \Xi^0 D_s^{*+}} \gamma_\mu (-g^{\mu\alpha} + \frac{p_4^\mu p_4^\alpha}{m_{D_s^{*+}}^2}) + \frac{f_{2\Xi_c^+ \Xi^0 D_s^{*+}}}{m_{\Xi_c^+} + m_{\Xi^0}} \sigma_{\mu\nu} i p_4^\mu (-g^{\nu\alpha} + \frac{p_4^\nu p_4^\alpha}{m_{D_s^{*+}}^2}) \right] \\
&\times (\not{p}_3 + m_{\Xi_c^+}) \left[ (m_{\Omega_{cc}^+} - m_{\Xi_c^+}) f_1(m_{\eta_1}^2) + (m_{\Omega_{cc}^+} + m_{\Xi_c^+}) g_1(m_{\eta_1}^2) \gamma_5 \right] u(p_1, s_z), \tag{20}
\end{aligned}$$

$$\begin{aligned}
Abs M_e(\eta_1; \Xi_c'^+; D_s^{*+}) &= - \int \frac{|\vec{p}_2| \sin\theta d\theta d\varphi}{32\pi^2 m_{\Omega_{cc}^+}} \frac{G_F}{\sqrt{2}} V_{cs}^* V_{us} a_2 f_{\eta_1} \frac{F^2(t, m_{D_s^{*+}})}{t - m_{D_s^{*+}}^2 + im_{D_s^{*+}} \Gamma_{D_s^{*+}}} g_{D_s^{*+} D_s^+ \eta_1} p_{2\alpha} \\
&\times \bar{u}(p_6, s'_z) \left[ f_{1\Xi_c'^+ \Xi^0 D_s^{*+}} \gamma_\mu (-g^{\mu\alpha} + \frac{p_4^\mu p_4^\alpha}{m_{D_s^{*+}}^2}) + \frac{f_{2\Xi_c'^+ \Xi^0 D_s^{*+}}}{m_{\Xi_c'^+} + m_{\Xi^0}} \sigma_{\mu\nu} i p_4^\mu (-g^{\nu\alpha} + \frac{p_4^\nu p_4^\alpha}{m_{D_s^{*+}}^2}) \right] \\
&\times (\not{p}_3 + m_{\Xi_c'^+}) \left[ (m_{\Omega_{cc}^+} - m_{\Xi_c'^+}) f_1(m_{\eta_1}^2) + (m_{\Omega_{cc}^+} + m_{\Xi_c'^+}) g_1(m_{\eta_1}^2) \gamma_5 \right] u(p_1, s_z), \tag{21}
\end{aligned}$$

$$\begin{aligned}
Abs M_e(\eta_8; \Xi_c^+; D_s^{*+}) &= - \int \frac{|\vec{p}_2| \sin\theta d\theta d\varphi}{32\pi^2 m_{\Omega_{cc}^+}} \frac{G_F}{\sqrt{2}} V_{cs}^* V_{us} a_2 f_{\eta_8} \frac{F^2(t, m_{D_s^{*+}})}{t - m_{D_s^{*+}}^2 + im_{D_s^{*+}} \Gamma_{D_s^{*+}}} g_{D_s^{*+} D_s^+ \eta_8} p_{2\alpha} \\
&\times \bar{u}(p_6, s'_z) \left[ f_{1\Xi_c^+ \Xi^0 D_s^{*+}} \gamma_\mu (-g^{\mu\alpha} + \frac{p_4^\mu p_4^\alpha}{m_{D_s^{*+}}^2}) + \frac{f_{2\Xi_c^+ \Xi^0 D_s^{*+}}}{m_{\Xi_c^+} + m_{\Xi^0}} \sigma_{\mu\nu} i p_4^\mu (-g^{\nu\alpha} + \frac{p_4^\nu p_4^\alpha}{m_{D_s^{*+}}^2}) \right] \\
&\times (\not{p}_3 + m_{\Xi_c^+}) \left[ (m_{\Omega_{cc}^+} - m_{\Xi_c^+}) f_1(m_{\eta_8}^2) + (m_{\Omega_{cc}^+} + m_{\Xi_c^+}) g_1(m_{\eta_8}^2) \gamma_5 \right] u(p_1, s_z), \tag{22}
\end{aligned}$$

$$\begin{aligned}
Abs M_e(\eta_8; \Xi_c'^+; D_s^{*+}) &= - \int \frac{|\vec{p}_2| \sin\theta d\theta d\varphi}{32\pi^2 m_{\Omega_{cc}^+}} \frac{G_F}{\sqrt{2}} V_{cs}^* V_{us} a_2 f_{\eta_8} \frac{F^2(t, m_{D_s^{*+}})}{t - m_{D_s^{*+}}^2 + im_{D_s^{*+}} \Gamma_{D_s^{*+}}} g_{D_s^{*+} D_s^+ \eta_8} p_{2\alpha} \\
&\times \bar{u}(p_6, s'_z) \left[ f_{1\Xi_c'^+ \Xi^0 D_s^{*+}} \gamma_\mu (-g^{\mu\alpha} + \frac{p_4^\mu p_4^\alpha}{m_{D_s^{*+}}^2}) + \frac{f_{2\Xi_c'^+ \Xi^0 D_s^{*+}}}{m_{\Xi_c'^+} + m_{\Xi^0}} \sigma_{\mu\nu} i p_4^\mu (-g^{\nu\alpha} + \frac{p_4^\nu p_4^\alpha}{m_{D_s^{*+}}^2}) \right] \\
&\times (\not{p}_3 + m_{\Xi_c'^+}) \left[ (m_{\Omega_{cc}^+} - m_{\Xi_c'^+}) f_1(m_{\eta_8}^2) + (m_{\Omega_{cc}^+} + m_{\Xi_c'^+}) g_1(m_{\eta_8}^2) \gamma_5 \right] u(p_1, s_z), \tag{23}
\end{aligned}$$

$$\begin{aligned}
Abs M_c(\phi; \Xi_c^+; \Xi^0) &= -i \int \frac{|\vec{p}_2| \sin\theta d\theta d\varphi}{32\pi^2 m_{\Omega_{cc}^+}} \frac{G_F}{\sqrt{2}} V_{cs}^* V_{us} a_2 f_\phi \frac{F^2(t, m_{\Xi^0})}{t - m_{\Xi^0}^2 + im_{\Xi^0} \Gamma_{\Xi^0}} g_{\Xi_c^+ \Xi^0 D_s^+} \\
&\times \bar{u}(p_5, s'_z) \left[ f_{1\Xi^0 \Xi^0 \phi} \gamma_\mu (-g^{\alpha\mu} + \frac{p_2^\alpha p_2^\mu}{m_\phi^2}) + \frac{f_{2\Xi^0 \Xi^0 \phi}}{m_{\Xi^0} + m_{\Xi^0}} \sigma_{\mu\nu} (-ip_2^\mu) (-g^{\alpha\nu} + \frac{p_2^\alpha p_2^\nu}{m_\phi^2}) \right] \\
&\times (\not{p}_4 + m_{\Xi^0}) \gamma_5 (\not{p}_3 + m_{\Xi_c^+}) \left[ \left( f_1(m_\phi^2) - \frac{m_{\Omega_{cc}^+} + m_{\Xi_c^+}}{m_{\Omega_{cc}^+}} f_2(m_\phi^2) \right) \gamma_\alpha + \frac{2}{m_{\Omega_{cc}^+}} f_2(m_\phi^2) p_{3\alpha} \right. \\
&\left. - \left( g_1(m_\phi^2) + \frac{m_{\Omega_{cc}^+} - m_{\Xi_c^+}}{m_{\Omega_{cc}^+}} g_2(m_\phi^2) \right) \gamma_\alpha \gamma_5 - \frac{2}{m_{\Omega_{cc}^+}} g_2(m_\phi^2) p_{3\alpha} \gamma_5 \right] u(p_1, s_z). \tag{24}
\end{aligned}$$

$$\begin{aligned}
Abs M_c(\phi; \Xi_c'^+; \Xi^0) &= -i \int \frac{|\vec{p}_2| \sin\theta d\theta d\varphi}{32\pi^2 m_{\Omega_{cc}^+}} \frac{G_F}{\sqrt{2}} V_{cs}^* V_{us} a_2 f_\phi \frac{F^2(t, m_{\Xi^0})}{t - m_{\Xi^0}^2 + im_{\Xi^0} \Gamma_{\Xi^0}} g_{\Xi_c'^+ \Xi^0 D_s^+} \\
&\times \bar{u}(p_5, s'_z) \left[ f_{1\Xi^0 \Xi^0 \phi} \gamma_\mu (-g^{\alpha\mu} + \frac{p_2^\alpha p_2^\mu}{m_\phi^2}) + \frac{f_{2\Xi^0 \Xi^0 \phi}}{m_{\Xi^0} + m_{\Xi^0}} \sigma_{\mu\nu} (-ip_2^\mu) (-g^{\alpha\nu} + \frac{p_2^\alpha p_2^\nu}{m_\phi^2}) \right] \\
&\times (\not{p}_4 + m_{\Xi^0}) \gamma_5 (\not{p}_3 + m_{\Xi_c'^+}) \left[ \left( f_1(m_\phi^2) - \frac{m_{\Omega_{cc}^+} + m_{\Xi_c'^+}}{m_{\Omega_{cc}^+}} f_2(m_\phi^2) \right) \gamma_\alpha + \frac{2}{m_{\Omega_{cc}^+}} f_2(m_\phi^2) p_{3\alpha} \right. \\
&\left. - \left( g_1(m_\phi^2) + \frac{m_{\Omega_{cc}^+} - m_{\Xi_c'^+}}{m_{\Omega_{cc}^+}} g_2(m_\phi^2) \right) \gamma_\alpha \gamma_5 - \frac{2}{m_{\Omega_{cc}^+}} g_2(m_\phi^2) p_{3\alpha} \gamma_5 \right] u(p_1, s_z). \tag{25}
\end{aligned}$$

$$\begin{aligned}
Abs M_c(\eta_1; \Xi_c^+; \Xi^0) &= i \int \frac{|\vec{p}_2| \sin\theta d\theta d\varphi}{32\pi^2 m_{\Omega_{cc}^+}} \frac{G_F}{\sqrt{2}} V_{cs}^* V_{us} a_2 f_{\eta_1} \frac{F^2(t, m_{\Xi^0})}{t - m_{\Xi^0}^2 + im_{\Xi^0} \Gamma_{\Xi^0}} g_{\Xi^0 \Xi^0 \eta_1} g_{\Xi_c^+ \Xi^0 D_s^+} \\
&\times \bar{u}(p_5, s'_z) \gamma_5 (\not{p}_4 + m_{\Xi^0}) \gamma_5 (\not{p}_3 + m_{\Xi_c^+}) \\
&\times \left[ (m_{\Omega_{cc}^+} - m_{\Xi_c^+}) f_1(m_{\eta_1}^2) + (m_{\Omega_{cc}^+} + m_{\Xi_c^+}) g_1(m_{\eta_1}^2) \gamma_5 \right] u(p_1, s_z). \tag{26}
\end{aligned}$$

$$\begin{aligned}
Abs M_c(\eta_1; \Xi_c'^+; \Xi^0) &= i \int \frac{|\vec{p}_2| \sin\theta d\theta d\varphi}{32\pi^2 m_{\Omega_{cc}^+}} \frac{G_F}{\sqrt{2}} V_{cs}^* V_{us} a_2 f_{\eta_1} \frac{F^2(t, m_{\Xi^0})}{t - m_{\Xi^0}^2 + im_{\Xi^0} \Gamma_{\Xi^0}} g_{\Xi^0 \Xi^0 \eta_1} g_{\Xi_c'^+ \Xi^0 D_s^+} \\
&\times \bar{u}(p_5, s'_z) \gamma_5 (\not{p}_4 + m_{\Xi^0}) \gamma_5 (\not{p}_3 + m_{\Xi_c'^+}) \\
&\times \left[ (m_{\Omega_{cc}^+} - m_{\Xi_c'^+}) f_1(m_{\eta_1}^2) + (m_{\Omega_{cc}^+} + m_{\Xi_c'^+}) g_1(m_{\eta_1}^2) \gamma_5 \right] u(p_1, s_z). \tag{27}
\end{aligned}$$

$$\begin{aligned}
Abs M_c(\eta_8; \Xi_c^+; \Xi^0) &= i \int \frac{|\vec{p}_2| \sin\theta d\theta d\varphi}{32\pi^2 m_{\Omega_{cc}^+}} \frac{G_F}{\sqrt{2}} V_{cs}^* V_{us} a_2 f_{\eta_8} \frac{F^2(t, m_{\Xi^0})}{t - m_{\Xi^0}^2 + im_{\Xi^0} \Gamma_{\Xi^0}} g_{\Xi^0 \Xi^0 \eta_8} g_{\Xi_c^+ \Xi^0 D_s^+} \\
&\times \bar{u}(p_5, s'_z) \gamma_5 (\not{p}_4 + m_{\Xi^0}) \gamma_5 (\not{p}_3 + m_{\Xi_c^+}) \\
&\times \left[ (m_{\Omega_{cc}^+} - m_{\Xi_c^+}) f_1(m_{\eta_8}^2) + (m_{\Omega_{cc}^+} + m_{\Xi_c^+}) g_1(m_{\eta_8}^2) \gamma_5 \right] u(p_1, s_z). \tag{28}
\end{aligned}$$

$$\begin{aligned}
Abs M_c(\eta_8; \Xi_c'^+; \Xi^0) &= i \int \frac{|\vec{p}_2| \sin\theta d\theta d\varphi}{32\pi^2 m_{\Omega_{cc}^+}} \frac{G_F}{\sqrt{2}} V_{cs}^* V_{us} a_2 f_{\eta_8} \frac{F^2(t, m_{\Xi^0})}{t - m_{\Xi^0}^2 + im_{\Xi^0} \Gamma_{\Xi^0}} g_{\Xi^0 \Xi^0 \eta_8} g_{\Xi_c'^+ \Xi^0 D_s^+} \\
&\times \bar{u}(p_5, s'_z) \gamma_5 (\not{p}_4 + m_{\Xi^0}) \gamma_5 (\not{p}_3 + m_{\Xi_c'^+}) \\
&\times \left[ (m_{\Omega_{cc}^+} - m_{\Xi_c'^+}) f_1(m_{\eta_8}^2) + (m_{\Omega_{cc}^+} + m_{\Xi_c'^+}) g_1(m_{\eta_8}^2) \gamma_5 \right] u(p_1, s_z). \tag{29}
\end{aligned}$$

$$\begin{aligned}
Abs M_f(\pi^+; \Xi_c^0; \Xi^-) &= i \int \frac{|\vec{p}_2| \sin\theta d\theta d\varphi}{32\pi^2 m_{\Omega_{cc}^+}} \frac{G_F}{\sqrt{2}} V_{cd}^* V_{ud} a_2 f_{\pi^+} \frac{F^2(t, m_{\Xi^-})}{t - m_{\Xi^-}^2 + im_{\Xi^-} \Gamma_{\Xi^-}} g_{\Xi^0 \Xi^- \pi^+} g_{\Xi_c^0 \Xi^- D_s^+} \\
&\times \bar{u}(p_5, s'_z) \gamma_5 (\not{p}_4 + m_{\Xi^-}) \gamma_5 (\not{p}_3 + m_{\Xi_c^0}) \\
&\times \left[ (m_{\Omega_{cc}^+} - m_{\Xi_c^0}) f_1(m_{\pi^+}^2) + (m_{\Omega_{cc}^+} + m_{\Xi_c^0}) g_1(m_{\pi^+}^2) \gamma_5 \right] u(p_1, s_z). \tag{30}
\end{aligned}$$



$$\begin{aligned}
Abs M_f(\pi^+; \Xi_c^{\prime 0}; \Xi^-) &= i \int \frac{|\vec{p}_2| \sin\theta d\theta d\varphi}{32\pi^2 m_{\Omega_{cc}^+}} \frac{G_F}{\sqrt{2}} V_{cd}^* V_{ud} a_2 f_{\pi^+} \frac{F^2(t, m_{\Xi^-})}{t - m_{\Xi^-}^2 + im_{\Xi^-} \Gamma_{\Xi^-}} g_{\Xi^0 \Xi^- \pi^+} g_{\Xi_c^{\prime 0} \Xi^- D_s^+} \\
&\times \bar{u}(p_5, s'_z) \gamma_5 (\not{p}_4 + m_{\Xi^-}) \gamma_5 (\not{p}_3 + m_{\Xi_c^{\prime 0}}) \\
&\times \left[ (m_{\Omega_{cc}^+} - m_{\Xi_c^{\prime 0}}) f_1(m_{\pi^+}^2) + (m_{\Omega_{cc}^+} + m_{\Xi_c^{\prime 0}}) g_1(m_{\pi^+}^2) \gamma_5 \right] u(p_1, s_z). \tag{31}
\end{aligned}$$

$$\begin{aligned}
Abs M_f(\rho^+; \Xi_c^0; \Xi^-) &= -i \int \frac{|\vec{p}_2| \sin\theta d\theta d\varphi}{32\pi^2 m_{\Omega_{cc}^+}} \frac{G_F}{\sqrt{2}} V_{cd}^* V_{ud} a_2 f_{\rho^+} \frac{F^2(t, m_{\Xi^-})}{t - m_{\Xi^-}^2 + im_{\Xi^-} \Gamma_{\Xi^-}} g_{\Xi_c^0 \Xi^- D_s^+} \\
&\times \bar{u}(p_5, s'_z) \left[ f_{1\Xi^0 \Xi^- \rho^+} \gamma_\mu + \frac{f_{2\Xi^0 \Xi^- \rho^+}}{m_{\Xi^0} + m_{\Xi^-}} \sigma_{\mu\nu} (-ip_2^\mu) \right] \\
&\times (\not{p}_4 + m_{\Xi^-}) \gamma_5 (\not{p}_3 + m_{\Xi_c^0}) (-g^{\alpha\mu} + \frac{p_2^\alpha p_2^\mu}{m_{\rho^+}^2}) (-g^{\alpha\nu} + \frac{p_2^\alpha p_2^\nu}{m_{\rho^+}^2}) \\
&\times \left[ \left( f_1(m_{\rho^+}^2) - \frac{m_{\Omega_{cc}^+} + m_{\Xi_c^0}}{m_{\Omega_{cc}^+}} f_2(m_{\rho^+}^2) \right) \gamma_\alpha + \frac{2}{m_{\Omega_{cc}^+}} f_2(m_{\rho^+}^2) p_{3\alpha} \right. \\
&\left. - \left( g_1(m_{\rho^+}^2) + \frac{m_{\Omega_{cc}^+} - m_{\Xi_c^0}}{m_{\Omega_{cc}^+}} g_2(m_{\rho^+}^2) \right) \gamma_\alpha \gamma_5 - \frac{2}{m_{\Omega_{cc}^+}} g_2(m_{\rho^+}^2) p_{3\alpha} \gamma_5 \right] u(p_1, s_z). \tag{32}
\end{aligned}$$

$$\begin{aligned}
Abs M_f(\rho^+; \Xi_c^{\prime 0}; \Xi^-) &= -i \int \frac{|\vec{p}_2| \sin\theta d\theta d\varphi}{32\pi^2 m_{\Omega_{cc}^+}} \frac{G_F}{\sqrt{2}} V_{cd}^* V_{ud} a_2 f_{\rho^+} \frac{F^2(t, m_{\Xi^-})}{t - m_{\Xi^-}^2 + im_{\Xi^-} \Gamma_{\Xi^-}} g_{\Xi_c^{\prime 0} \Xi^- D_s^+} \\
&\times \bar{u}(p_5, s'_z) \left[ f_{1\Xi^0 \Xi^- \rho^+} \gamma_\mu + \frac{f_{2\Xi^0 \Xi^- \rho^+}}{m_{\Xi^0} + m_{\Xi^-}} \sigma_{\mu\nu} (-ip_2^\mu) \right] \\
&\times (\not{p}_4 + m_{\Xi^-}) \gamma_5 (\not{p}_3 + m_{\Xi_c^{\prime 0}}) (-g^{\alpha\mu} + \frac{p_2^\alpha p_2^\mu}{m_{\rho^+}^2}) (-g^{\alpha\nu} + \frac{p_2^\alpha p_2^\nu}{m_{\rho^+}^2}) \\
&\times \left[ \left( f_1(m_{\rho^+}^2) - \frac{m_{\Omega_{cc}^+} + m_{\Xi_c^{\prime 0}}}{m_{\Omega_{cc}^+}} f_2(m_{\rho^+}^2) \right) \gamma_\alpha + \frac{2}{m_{\Omega_{cc}^+}} f_2(m_{\rho^+}^2) p_{3\alpha} \right. \\
&\left. - \left( g_1(m_{\rho^+}^2) + \frac{m_{\Omega_{cc}^+} - m_{\Xi_c^{\prime 0}}}{m_{\Omega_{cc}^+}} g_2(m_{\rho^+}^2) \right) \gamma_\alpha \gamma_5 - \frac{2}{m_{\Omega_{cc}^+}} g_2(m_{\rho^+}^2) p_{3\alpha} \gamma_5 \right] u(p_1, s_z). \tag{33}
\end{aligned}$$

With all the diagrams calculated above the amplitude of  $\Omega_{cc}^+ \rightarrow \Xi^0 D_s^+$  is given as

$$\begin{aligned}
\mathcal{A}(\Omega_{cc}^+ \rightarrow \Xi^0 D_s^+) &= i Abs [ M_a(K^+; \Omega_c^0; D^{*0}) + M_b(\phi; \Xi_c^+; D_s^+) + M_b(\phi; \Xi_c^{\prime+}; D_s^+) + M_c(\phi; \Xi_c^+; \Xi^0) \\
&+ M_c(\phi; \Xi_c^{\prime+}; \Xi^0) + M_c(\eta_1; \Xi_c^+; \Xi^0) + M_c(\eta_1; \Xi_c^{\prime+}; \Xi^0) + M_c(\eta_8; \Xi_c^+; \Xi^0) \\
&+ M_c(\eta_8; \Xi_c^{\prime+}; \Xi^0) + M_d(K^{*+}; \Omega_c^0; D^0) + M_e(\eta_1; \Xi_c^+; D_s^{*+}) + M_e(\eta_1; \Xi_c^{\prime+}; D_s^{*+}) \\
&+ M_e(\eta_8; \Xi_c^+; D_s^{*+}) + M_e(\eta_8; \Xi_c^{\prime+}; D_s^{*+}) + M_f(\pi^+; \Xi_c^0; \Xi^-) + M_f(\pi^+; \Xi_c^{\prime 0}; \Xi^-) \\
&+ M_f(\rho^+; \Xi_c^0; \Xi^-) + M_f(\rho^+; \Xi_c^{\prime 0}; \Xi^-) ]. \tag{34}
\end{aligned}$$

The amplitudes of the other decays can be obtained in the same way. For shortage of the paper, we collect these expressions in appendix A.

### III. NUMERICAL RESULTS AND DISCUSSIONS

The decay width of  $\mathcal{B}_{cc} \rightarrow \mathcal{B}D^{(*)}$  can be calculated at the rest frame of  $\mathcal{B}_{cc}$  by

$$\Gamma(\mathcal{B}_{cc} \rightarrow \mathcal{B}D^{(*)}) = \frac{\sqrt{(m_{\mathcal{B}_{cc}}^2 - (m_{\mathcal{B}} + m_{D^{(*)}})^2)((m_{\mathcal{B}_{cc}}^2 - (m_{\mathcal{B}} - m_{D^{(*)}})^2)}{32\pi m_{\mathcal{B}_{cc}}^3} \sum_{\text{pol.}} |\mathcal{A}(\mathcal{B}_{cc} \rightarrow \mathcal{B}D^{(*)})|^2, \tag{35}$$

where the summations are performed over the polarizations of initial and final states. In addition a factor 1/2 has already been multiplied to average over the polarizations of the mother particle  $\mathcal{B}_{cc}$ .

TABLE I: Decay constants of light pseudoscalar and vector mesons collected from Refs. [42, 43] (in unit of MeV).  $f_{\eta_8}$  and  $f_{\eta_1}$  are calculated with the formulas in Ref. [41]

$f_\pi$	$f_K$	$f_{\eta_8}$	$f_{\eta_1}$	$f_\rho$	$f_{K^*}$	$f_\omega$	$f_\phi$
130	156	163	152	216	217	195	233

The calculation of the short distance contribution needs the decay constants of some pseudoscalar and vector mesons, which are gathered in table I. Besides, large amount of strong couplings are in need. Most of them are from Refs. [28, 34–40]. There are still some ones that can not be found in the literature, and they are calculated under the  $SU(3)_F$  symmetry. For shortage of the paper, the data for strong couplings are listed in the appendix B.

TABLE II: Our results for branching ratios of  $\Xi_{cc}^{++} \rightarrow \mathcal{B}D^{(*)}$ . The ‘‘CF’’, ‘‘SCS’’ and ‘‘DCS’’ represent CKM favored, singly CKM suppressed and doubly CKM suppressed processes, respectively. The errors are estimated by varying  $\eta$  from 1 to 2, and the central values are given at  $\eta = 1.5$

Channels	$\mathcal{BR}(10^{-3})$	CKM	Channels	$\mathcal{BR}(10^{-3})$	CKM
$\Xi_{cc}^{++} \rightarrow \Sigma^+ D^+$	$2.98_{-2.02}^{+3.16}$	CF	$\Xi_{cc}^{++} \rightarrow \Sigma^+ D^{*+}$	$16.06_{-10.50}^{+17.28}$	CF
$\Xi_{cc}^{++} \rightarrow \Sigma^+ D_s^+$	$0.17_{-0.12}^{+0.18}$	SCS	$\Xi_{cc}^{++} \rightarrow \Sigma^+ D_s^{*+}$	$2.68_{-1.71}^{+2.64}$	SCS
$\Xi_{cc}^{++} \rightarrow p D^+$	$0.16_{-0.11}^{+0.18}$	SCS	$\Xi_{cc}^{++} \rightarrow p D^{*+}$	$2.96_{-2.06}^{+3.38}$	SCS
$\Xi_{cc}^{++} \rightarrow p D_s^+$	$0.01_{-0.00}^{+0.02}$	DCS	$\Xi_{cc}^{++} \rightarrow p D_s^{*+}$	$0.11_{-0.07}^{+0.13}$	DCS

With all the ingredients ready we can obtain the numerical values for related decays. We use the lifetime  $\tau_{\Xi_{cc}^{++}} = 256$  fs [4] measured by the LHCb collaboration to calculate the branching fractions of  $\Xi_{cc}^{++}$  decays, and the results are collected in table II. One can see that the branching ratios of  $\Xi_{cc}^{++} \rightarrow \mathcal{B}D^*$  decays tend to be larger than those of  $\Xi_{cc}^{++} \rightarrow \mathcal{B}D$  mode with the same quark constituents. It’s can be easily understood that the  $\Xi_{cc}^{++} \rightarrow \mathcal{B}D^*$  decays receive contributions of more polarization states. Among these decays the CKM favored ones have the largest branching ratios doubtlessly. The branching ratio of  $\Xi_{cc}^{++} \rightarrow \Sigma^+ D^{*+}$  is estimated to reach the percentage level.

TABLE III: The same as table II but for decay widths of  $\Xi_{cc}^+ \rightarrow \mathcal{B}D^{(*)}$

Channels	$\Gamma/\text{GeV}$	CKM	Channels	$\Gamma/\text{GeV}$	CKM
$\Xi_{cc}^+ \rightarrow \Sigma^0 D^+$	$(5.93_{-4.05}^{+6.31}) * 10^{-15}$	CF	$\Xi_{cc}^+ \rightarrow \Lambda D^{*+}$	$(1.82_{-1.26}^{+2.03}) * 10^{-13}$	CF
$\Xi_{cc}^+ \rightarrow \Lambda D^+$	$(5.84_{-3.98}^{+6.16}) * 10^{-15}$	CF	$\Xi_{cc}^+ \rightarrow \Sigma^0 D^{*+}$	$(2.17_{-1.51}^{+2.45}) * 10^{-13}$	CF
$\Xi_{cc}^+ \rightarrow \Sigma^+ D^0$	$(1.23_{-0.77}^{+1.24}) * 10^{-15}$	CF	$\Xi_{cc}^+ \rightarrow \Sigma^+ D^{*0}$	$(6.77_{-4.46}^{+7.37}) * 10^{-14}$	CF
$\Xi_{cc}^+ \rightarrow \Xi^0 D_s^+$	$(4.52_{-3.49}^{+5.22}) * 10^{-16}$	CF	$\Xi_{cc}^+ \rightarrow \Xi^0 D_s^{*+}$	$(2.52_{-1.48}^{+2.23}) * 10^{-14}$	CF
$\Xi_{cc}^+ \rightarrow p D^0$	$(1.85_{-1.27}^{+2.02}) * 10^{-15}$	SCS	$\Xi_{cc}^+ \rightarrow \Sigma^0 D_s^{*+}$	$(1.15_{-0.85}^{+1.41}) * 10^{-14}$	SCS
$\Xi_{cc}^+ \rightarrow \Lambda D_s^+$	$(3.00_{-2.00}^{+2.93}) * 10^{-16}$	SCS	$\Xi_{cc}^+ \rightarrow \Lambda D_s^{*+}$	$(1.58_{-1.09}^{+1.73}) * 10^{-14}$	SCS
$\Xi_{cc}^+ \rightarrow n D^+$	$(1.59_{-1.13}^{+1.87}) * 10^{-16}$	SCS	$\Xi_{cc}^+ \rightarrow n D^{*+}$	$(1.04_{-0.87}^{+1.41}) * 10^{-15}$	SCS
$\Xi_{cc}^+ \rightarrow \Sigma^0 D_s^+$	$(2.85_{-1.78}^{+2.72}) * 10^{-16}$	SCS	$\Xi_{cc}^+ \rightarrow p D^{*0}$	$(9.46_{-6.49}^{+10.20}) * 10^{-15}$	SCS
$\Xi_{cc}^+ \rightarrow n D_s^+$	$(3.26_{-2.41}^{+3.88}) * 10^{-17}$	DCS	$\Xi_{cc}^+ \rightarrow n D_s^{*+}$	$(1.47_{-1.00}^{+1.57}) * 10^{-16}$	DCS

Instead of the branching ratios the decay widths of  $\Xi_{cc}^+$  and  $\Omega_{cc}^+$  decays are presented in tables III and IV, because there is no experimental data for their lifetimes. Among decays of the same mode,  $\mathcal{B}_{cc} \rightarrow \mathcal{B}D$  or  $\mathcal{B}_{cc} \rightarrow \mathcal{B}D^*$ , the CKM favored, singly CKM suppressed and doubly CKM suppressed decays fall into a hierarchy naturally. One can also see that in table III, some singly CKM suppressed  $\Xi_{cc}^+ \rightarrow \mathcal{B}D^*$  decays even have larger decay widths than the CKM favored  $\Xi_{cc}^+ \rightarrow \mathcal{B}D$  ones’.  $\Xi_{cc}^+ \rightarrow \Lambda D^{*+}$  and  $\Xi_{cc}^+ \rightarrow \Sigma^0 D^{*+}$  own the largest decay widths among  $\Xi_{cc}^+ \rightarrow \mathcal{B}D^{(*)}$  decays. Estimated with a recent calculated lifetime  $\tau_{\Xi_{cc}^+} = 45$  fs in Ref. [44], their branching ratios are given by

$$\begin{aligned} \mathcal{BR}(\Xi_{cc}^+ \rightarrow \Lambda D^{*+}) &\in [0.38\%, 2.63\%], \\ \mathcal{BR}(\Xi_{cc}^+ \rightarrow \Sigma^0 D^{*+}) &\in [0.45\%, 3.16\%]. \end{aligned} \quad (36)$$

The lifetime of  $\Omega_{cc}^+$  is predicted to lies in the range  $75 \sim 180$  fs in Ref. [44]. Here we use the boundary 75 fs to

TABLE IV: The same as table II but for decay widths of  $\Omega_{cc}^+ \rightarrow \mathcal{B}D^{(*)}$ 

Channels	$\Gamma/\text{GeV}$	CKM	Channels	$\Gamma/\text{GeV}$	CKM
$\Omega_{cc}^+ \rightarrow \Xi^0 D^+$	$(1.88_{-1.25}^{+1.97}) * 10^{-14}$	CF	$\Omega_{cc}^+ \rightarrow \Xi^0 D^{*+}$	$(4.99_{-2.62}^{+4.05}) * 10^{-14}$	CF
$\Omega_{cc}^+ \rightarrow \Sigma^+ D^0$	$(1.76_{-1.07}^{+1.71}) * 10^{-15}$	SCS	$\Omega_{cc}^+ \rightarrow \Sigma^0 D^{*+}$	$(1.80_{-1.27}^{+2.14}) * 10^{-14}$	SCS
$\Omega_{cc}^+ \rightarrow \Lambda D^+$	$(1.75_{-1.21}^{+1.98}) * 10^{-15}$	SCS	$\Omega_{cc}^+ \rightarrow \Lambda D^{*+}$	$(7.65_{-5.32}^{+8.69}) * 10^{-15}$	SCS
$\Omega_{cc}^+ \rightarrow \Xi^0 D_s^+$	$(9.93_{-6.84}^{+10.87}) * 10^{-16}$	SCS	$\Omega_{cc}^+ \rightarrow \Xi^0 D_s^{*+}$	$(4.26_{-2.81}^{+4.06}) * 10^{-16}$	SCS
$\Omega_{cc}^+ \rightarrow \Sigma^0 D^+$	$(2.37_{-1.20}^{+2.14}) * 10^{-16}$	SCS	$\Omega_{cc}^+ \rightarrow \Sigma^+ D^{*0}$	$(6.91_{-4.15}^{+6.24}) * 10^{-15}$	SCS
$\Omega_{cc}^+ \rightarrow \Sigma^0 D_s^+$	$(1.17_{-6.57}^{+10.93}) * 10^{-16}$	DCS	$\Omega_{cc}^+ \rightarrow \Sigma^0 D_s^{*+}$	$(1.68_{-1.18}^{+1.92}) * 10^{-16}$	DCS
$\Omega_{cc}^+ \rightarrow p D^0$	$(1.74_{-1.23}^{+2.05}) * 10^{-17}$	DCS	$\Omega_{cc}^+ \rightarrow p D^{*0}$	$(3.83_{-2.74}^{+4.85}) * 10^{-16}$	DCS
$\Omega_{cc}^+ \rightarrow n D^+$	$(4.32_{-3.30}^{+5.56}) * 10^{-17}$	DCS	$\Omega_{cc}^+ \rightarrow \Lambda D_s^{*+}$	$(1.06_{-0.75}^{+1.27}) * 10^{-16}$	DCS
$\Omega_{cc}^+ \rightarrow \Lambda D_s^+$	$(7.00_{-4.85}^{+7.87}) * 10^{-18}$	DCS	$\Omega_{cc}^+ \rightarrow n D^{*+}$	$(2.74_{-2.09}^{+3.29}) * 10^{-17}$	DCS

estimate the three largest branching fractions in  $\Omega_{cc}^+ \rightarrow \mathcal{B}D^{(*)}$  decays, which are given as

$$\begin{aligned}
\mathcal{BR}(\Omega_{cc}^+ \rightarrow \Xi^0 D^{*+}) &\in [0.27\%, 1.03\%], \\
\mathcal{BR}(\Omega_{cc}^+ \rightarrow \Xi^0 D^+) &\in [0.07\%, 0.44\%], \\
\mathcal{BR}(\Omega_{cc}^+ \rightarrow \Sigma^0 D^{*+}) &\in [0.06\%, 0.45\%].
\end{aligned} \tag{37}$$

Although most of the decays have small branching fractions, some ones can reach the percentage level. It indicates that at the charm scale the bow tie topology dynamics may also be important and can not be neglected easily.

#### IV. SUMMARY

The discovery of  $\Xi_{cc}^{++}$  in 2017 inspires the interest of studying doubly charmed baryons. Among all the topics, how to calculate their weak decays is a meaningful and challenging one. It can give valuable suggestions for experimental searches as well as helps to understand the dynamics in baryon decays. In our previous work we apply the model of final state interactions to baryon decays and realize the calculation of two body nonleptonic decays of charm baryons.

In this paper we calculate the decays of a doubly charmed baryon to a light baryon and a charm meson. In the same decay mode,  $\mathcal{B}_{cc} \rightarrow \mathcal{B}D$  or  $\mathcal{B}_{cc} \rightarrow \mathcal{B}D^*$ , the CKM favored, singly CKM suppressed and doubly CKM suppressed decays fall into a hierarchy naturally. The  $\mathcal{B}_{cc} \rightarrow \mathcal{B}D^*$  decays tends to have larger branching ratios or decay widths since they receives more contributions from polarization states.  $\Xi_{cc}^{++} \rightarrow \Sigma^+ D^{*+}$  has the largest branching ratio in  $\Xi_{cc}^{++} \rightarrow \mathcal{B}D^{(*)}$  decays, which lies in  $(0.46 \sim 3.33)\%$ . The two largest branching ratios in  $\Xi_{cc}^+ \rightarrow \mathcal{B}D^{(*)}$  mode are  $\mathcal{BR}(\Xi_{cc}^+ \rightarrow \Lambda D^{*+}) \in [0.38\%, 2.63\%]$  and  $\mathcal{BR}(\Xi_{cc}^+ \rightarrow \Sigma^0 D^{*+}) \in [0.45\%, 3.16\%]$ , which are estimated with  $\tau_{\Xi_{cc}^+} = 45$  fs. For  $\Omega_{cc}^+ \rightarrow \mathcal{B}D^{(*)}$  mode  $\mathcal{BR}(\Omega_{cc}^+ \rightarrow \Xi^0 D^{*+}) \in [0.27\%, 1.03\%]$ ,  $\mathcal{BR}(\Omega_{cc}^+ \rightarrow \Xi^0 D^+) \in [0.07\%, 0.44\%]$ , and  $\mathcal{BR}(\Omega_{cc}^+ \rightarrow \Sigma^0 D^{*+}) \in [0.06\%, 0.45\%]$  are three largest ones, and they are calculated with  $\tau_{\Omega_{cc}^+} = 75$  fs.

All the decays calculated in this paper are pure bow tie topology processes. One can see that some branching ratios can reach the percentage level. It indicates that the bow tie topology may also play an important role at the charm scale just like the  $W$  exchange topology.

#### V. ACKNOWLEDGEMENT

This work is supported by the National Natural Science Foundation of China under the Grant Nos. 11765012 and 11505098. We would like to thank Z.-T. Zou for helpful discussions.

#### Appendix A: Expressions of Amplitudes

The expressions of amplitudes for all the  $\mathcal{B}_{cc} \rightarrow \mathcal{B}D^{(*)}$  decays are collected in this section. In order to make the expressions simpler, we define a function  $\mathcal{M}(P1, P2, P3, P4, P5, P6)$  to represent the absorptive part of a triangle diagram shown in Fig. 4. The absorptive part in Eq. (14) is related to this function by

$$\text{Abs } M_a(K^+; \Omega_c^0; D^{*0}) = \mathcal{M}(\Omega_{cc}^+, K^+, \Omega_c^0, D^{*0}, \Xi^0, D_s^+). \tag{A1}$$

















$$\begin{aligned}
\mathcal{A}(\Omega_{cc}^+ \rightarrow nD^+) &= i[\mathcal{M}(\Omega_{cc}^+, K^+, \Xi_c^0, \Sigma^-, n, D^+) + \mathcal{M}(\Omega_{cc}^+, K^+, \Xi_c'^0, \Sigma^-, n, D^+) + \mathcal{M}(\Omega_{cc}^+, K^{*+}, \Xi_c^0, \Sigma^-, n, D^+) \\
&\quad + \mathcal{M}(\Omega_{cc}^+, K^{*+}, \Xi_c'^0, \Sigma^-, n, D^+) + \mathcal{M}(\Omega_{cc}^+, K^0, \Xi_c^+, \Sigma^0, n, D^+) + \mathcal{M}(\Omega_{cc}^+, K^0, \Xi_c'^+, \Lambda, n, D^+) \\
&\quad + \mathcal{M}(\Omega_{cc}^+, K^0, \Xi_c'^+, \Sigma^0, n, D^+) + \mathcal{M}(\Omega_{cc}^+, K^0, \Xi_c'^+, \Lambda, n, D^+) + \mathcal{M}(\Omega_{cc}^+, K^{*0}, \Xi_c^+, \Sigma^0, n, D^+) \\
&\quad + \mathcal{M}(\Omega_{cc}^+, K^{*0}, \Xi_c'^+, \Lambda, n, D^+) + \mathcal{M}(\Omega_{cc}^+, K^{*0}, \Xi_c'^+, \Sigma^0, n, D^+) + \mathcal{M}(\Omega_{cc}^+, K^{*0}, \Xi_c'^+, \Lambda, n, D^+)], \tag{A44}
\end{aligned}$$

$$\begin{aligned}
\mathcal{A}(\Omega_{cc}^+ \rightarrow nD^{*+}) &= i[\mathcal{M}(\Omega_{cc}^+, K^+, \Xi_c^0, \Sigma^-, n, D^{*+}) + \mathcal{M}(\Omega_{cc}^+, K^+, \Xi_c'^0, \Sigma^-, n, D^{*+}) + \mathcal{M}(\Omega_{cc}^+, K^{*+}, \Xi_c^0, \Sigma^-, n, D^{*+}) \\
&\quad + \mathcal{M}(\Omega_{cc}^+, K^{*+}, \Xi_c'^0, \Sigma^-, n, D^{*+}) + \mathcal{M}(\Omega_{cc}^+, K^0, \Xi_c^+, \Sigma^0, n, D^{*+}) + \mathcal{M}(\Omega_{cc}^+, K^0, \Xi_c'^+, \Lambda, n, D^{*+}) \\
&\quad + \mathcal{M}(\Omega_{cc}^+, K^0, \Xi_c'^+, \Sigma^0, n, D^{*+}) + \mathcal{M}(\Omega_{cc}^+, K^0, \Xi_c'^+, \Lambda, n, D^{*+}) + \mathcal{M}(\Omega_{cc}^+, K^{*0}, \Xi_c^+, \Sigma^0, n, D^{*+}) \\
&\quad + \mathcal{M}(\Omega_{cc}^+, K^{*0}, \Xi_c'^+, \Lambda, n, D^{*+}) + \mathcal{M}(\Omega_{cc}^+, K^{*0}, \Xi_c'^+, \Sigma^0, n, D^{*+}) + \mathcal{M}(\Omega_{cc}^+, K^{*0}, \Xi_c'^+, \Lambda, n, D^{*+})], \tag{A45}
\end{aligned}$$

$$\begin{aligned}
\mathcal{A}(\Omega_{cc}^+ \rightarrow nD^{*+}) &= i[\mathcal{M}(\Omega_{cc}^+, K^+, \Xi_c^0, \Sigma^-, n, D^{*+}) + \mathcal{M}(\Omega_{cc}^+, K^+, \Xi_c'^0, \Sigma^-, n, D^{*+}) + \mathcal{M}(\Omega_{cc}^+, K^{*+}, \Xi_c^0, \Sigma^-, n, D^{*+}) \\
&\quad + \mathcal{M}(\Omega_{cc}^+, K^{*+}, \Xi_c'^0, \Sigma^-, n, D^{*+}) + \mathcal{M}(\Omega_{cc}^+, K^0, \Xi_c^+, \Sigma^0, n, D^{*+}) + \mathcal{M}(\Omega_{cc}^+, K^0, \Xi_c'^+, \Lambda, n, D^{*+}) \\
&\quad + \mathcal{M}(\Omega_{cc}^+, K^0, \Xi_c'^+, \Sigma^0, n, D^{*+}) + \mathcal{M}(\Omega_{cc}^+, K^0, \Xi_c'^+, \Lambda, n, D^{*+}) + \mathcal{M}(\Omega_{cc}^+, K^{*0}, \Xi_c^+, \Sigma^0, n, D^{*+}) \\
&\quad + \mathcal{M}(\Omega_{cc}^+, K^{*0}, \Xi_c'^+, \Lambda, n, D^{*+}) + \mathcal{M}(\Omega_{cc}^+, K^{*0}, \Xi_c'^+, \Sigma^0, n, D^{*+}) + \mathcal{M}(\Omega_{cc}^+, K^{*0}, \Xi_c'^+, \Lambda, n, D^{*+})]. \tag{A46}
\end{aligned}$$

## Appendix B: Strong Coupling Constants

In this section we list all the strong coupling constants used in our calculation. Some of these values are taken from Refs. [28, 34–40]. For those that can not be found directly in the literatures, we calculate them under the assumption of  $SU(3)_F$  symmetry.

According to which  $SU(3)_F$  multiplets do the particles belong to, the vertices in this paper can be divided into  $BBV$ ,  $BBP$ ,  $DD^*P$ ,  $DDV$ ,  $D^*D^*V$ ,  $\mathcal{B}_c\mathcal{B}D$  and  $\mathcal{B}_c\mathcal{B}D^*$ .  $P$  denotes a light pseudoscalar meson,  $V$  represents a light vector meson, and  $\mathcal{B}_c$  is a singly charmed baryon. With these label-definitions one can know the meaning of our symbols for each vertices whose coupling constants are collected in tables V, VI, VII, VIII.

TABLE V: Strong coupling constants of  $BBV$  vertices

vertex	$f_1$	$f_2$	vertex	$f_1$	$f_2$	vertex	$f_1$	$f_2$
$p \rightarrow n\rho^+$	-2.40	32.95	$\Lambda \rightarrow \Sigma^- \rho^+$	2.00	12.30	$\Sigma^0 \rightarrow \Sigma^+ \rho^+$	7.20	-25.00
$\Sigma^+ \rightarrow \Lambda\rho^+$	2.00	12.30	$\Sigma^+ \rightarrow p\bar{K}^{*0}$	5.66	-1.70	$\Sigma^+ \rightarrow \Xi^0 K^{*+}$	-2.26	37.05
$\Sigma^+ \rightarrow \Sigma^+ \phi$	-6.00	2.50	$p \rightarrow \Sigma^0 K^{*+}$	4.00	-1.20	$p \rightarrow \Lambda K^{*+}$	5.10	-28.00
$p \rightarrow \Sigma^+ K^{*0}$	5.66	-1.70	$\Sigma^0 \rightarrow \Sigma^- \rho^+$	-7.20	25.00	$\Sigma^0 \rightarrow n\bar{K}^{*0}$	-4.00	1.20
$\Lambda \rightarrow n\bar{K}^{*0}$	5.10	-28.00	$\Sigma^0 \rightarrow \Xi^- K^{*+}$	-1.60	26.20	$\Sigma^0 \rightarrow \Sigma^0 \phi$	-6.00	2.50
$\Sigma^0 \rightarrow \Sigma^0 \omega$	4.30	-1.10	$\Lambda \rightarrow \Sigma^0 \rho^0$	1.90	11.90	$p \rightarrow p\rho^0$	-2.50	22.20
$\Lambda \rightarrow \Xi^0 K^{*0}$	-6.00	17.10	$\Lambda \rightarrow \Xi^- K^{*+}$	-6.00	17.10	$\Lambda \rightarrow \Lambda\phi$	-5.30	24.60
$n \rightarrow \Sigma^0 K^{*0}$	-4.00	1.20	$\Lambda \rightarrow \Lambda\omega$	-7.10	8.70	$n \rightarrow \Sigma^- K^{*+}$	5.66	-1.70
$n \rightarrow \Lambda K^{*0}$	5.10	-28.00	$\Xi^- \rightarrow \Sigma^+ \bar{K}^{*0}$	-2.26	37.05	$n \rightarrow n\rho^0$	2.50	-22.20
$\Xi^0 \rightarrow \Lambda\bar{K}^{*0}$	4.45	-27.54	$\Xi^0 \rightarrow \Xi^- \rho^+$	6.08	-1.56	$\Xi^0 \rightarrow \Sigma^0 \bar{K}^{*0}$	1.60	-26.20
$\Xi^0 \rightarrow \Xi^0 \phi$	-9.50	32.30	$\Sigma^0 \rightarrow \Xi^0 K^{*0}$	1.60	-26.20			

- 
- [1] M. Mattson *et al.* [SELEX Collaboration], Phys. Rev. Lett. **89**, 112001 (2002) doi:10.1103/PhysRevLett.89.112001 [hep-ex/0208014].
- [2] A. Ocherashvili *et al.* [SELEX Collaboration], Phys. Lett. B **628**, 18 (2005) doi:10.1016/j.physletb.2005.09.043 [hep-ex/0406033].
- [3] R. Aaij *et al.* [LHCb Collaboration], Phys. Rev. Lett. **119**, no. 11, 112001 (2017) doi:10.1103/PhysRevLett.119.112001 [arXiv:1707.01621 [hep-ex]].

TABLE VI: Strong coupling constants of  $\mathcal{B}BP$  vertices

vertex	g	vertex	g	vertex	g
$p \rightarrow n\pi^+$	21.20	$\Lambda \rightarrow \Sigma^- \pi^+$	10.00	$\Sigma^0 \rightarrow \Sigma^+ \pi^+$	-10.70
$\Sigma^+ \rightarrow \Lambda\pi^+$	10.00	$\Sigma^+ \rightarrow p\bar{K}^0$	5.75	$\Sigma^+ \rightarrow \Xi^0 K^+$	19.80
$p \rightarrow \Sigma^0 K^+$	4.25	$p \rightarrow \Lambda K^+$	-13.50	$p \rightarrow \Sigma^+ K^0$	5.75
$\Sigma^- \rightarrow \Sigma^0 \pi^+$	10.70	$\Sigma^0 \rightarrow n\bar{K}^0$	-4.25	$\Xi^- \rightarrow \Sigma^+ \bar{K}^0$	19.80
$\Sigma^0 \rightarrow \Xi^- K^+$	14.00	$\Lambda \rightarrow \Xi^- K^+$	4.25	$\Lambda \rightarrow n\bar{K}^0$	-13.50
$p \rightarrow p\eta_8$	4.25	$n \rightarrow \Sigma^- K^+$	4.70	$p \rightarrow p\pi^0$	14.90
$p \rightarrow p\eta_1$	14.14	$n \rightarrow n\pi^0$	-14.90	$n \rightarrow \Sigma^0 K^0$	-4.25
$n \rightarrow \Lambda K^0$	-13.50	$\Xi^0 \rightarrow \Sigma^0 \bar{K}^0$	-14.00	$n \rightarrow n\eta_8$	4.25
$\Xi^0 \rightarrow \Xi^- \pi^+$	4.70	$\Lambda \rightarrow \Xi^0 K^0$	4.25	$n \rightarrow n\eta_1$	14.14
$\Sigma^0 \rightarrow \Xi^0 K^0$	-14.00	$\Sigma^0 \rightarrow \Sigma^0 \eta_8$	10.00	$\Xi^0 \rightarrow \Lambda \bar{K}^0$	4.25
$\Lambda \rightarrow \Sigma^0 \pi^0$	10.00	$\Sigma^0 \rightarrow \Sigma^0 \eta_1$	14.14	$\Xi^0 \rightarrow \Xi^0 \eta_8$	-13.50
$\Lambda \rightarrow \Lambda\eta_8$	-10.00	$\Sigma^+ \rightarrow \Sigma^+ \eta_8$	10.00	$\Xi^0 \rightarrow \Xi^0 \eta_1$	14.14
$\Lambda \rightarrow \Lambda\eta_1$	-14.14	$\Sigma^+ \rightarrow \Sigma^+ \eta_1$	14.14		

TABLE VII: Strong coupling constants of  $DD^*P$ ,  $DDV$  and  $D^*D^*V$  vertices

vertex	g	vertex	g	vertex	g	f
$D^* \rightarrow D\pi$	17.90	$D \rightarrow D\rho$	3.69	$D^* \rightarrow D^*\rho$	3.69	4.61

TABLE VIII: Strong coupling constants of  $\mathcal{B}_c\mathcal{B}D$  and  $\mathcal{B}_c\mathcal{B}D^*$  vertices

vertex	g	vertex	g	f
$\Lambda_c \rightarrow ND_q$	4.82	$\Lambda_c \rightarrow ND_q^*$	-5.80	3.60
$\Sigma_c \rightarrow ND_q$	3.78	$\Sigma_c \rightarrow ND_q^*$	11.21	4.64

- [4] R. Aaij *et al.* [LHCb Collaboration], Phys. Rev. Lett. **121**, no. 5, 052002 (2018) doi:10.1103/PhysRevLett.121.052002 [arXiv:1806.02744 [hep-ex]].
- [5] R. Aaij *et al.* [LHCb Collaboration], Phys. Rev. Lett. **121**, no. 16, 162002 (2018) doi:10.1103/PhysRevLett.121.162002 [arXiv:1807.01919 [hep-ex]].
- [6] D. Ebert, R. N. Faustov, V. O. Galkin and A. P. Martynenko, Phys. Rev. D **70**, 014018 (2004) Erratum: [Phys. Rev. D **77**, 079903 (2008)] doi:10.1103/PhysRevD.70.014018, 10.1103/PhysRevD.77.079903 [hep-ph/0404280].
- [7] D. Ebert, R. N. Faustov, V. O. Galkin and A. P. Martynenko, Phys. Atom. Nucl. **68**, 784 (2005) [Yad. Fiz. **68**, 817 (2005)]. doi:10.1134/1.1935012
- [8] C. Albertus, E. Hernandez, J. Nieves and J. M. Verde-Velasco, Eur. Phys. J. A **31**, 691 (2007) doi:10.1140/epja/i2006-10242-2 [hep-ph/0610131].
- [9] C. Albertus, E. Hernandez and J. Nieves, Phys. Rev. D **85**, 094035 (2012) doi:10.1103/PhysRevD.85.094035 [arXiv:1202.4861 [hep-ph]].
- [10] W. Wang, F. S. Yu and Z. X. Zhao, Eur. Phys. J. C **77**, no. 11, 781 (2017) doi:10.1140/epjc/s10052-017-5360-1 [arXiv:1707.02834 [hep-ph]].
- [11] X. H. Hu, Y. L. Shen, W. Wang and Z. X. Zhao, Chin. Phys. C **42**(12),123102(2018), doi:10.1088/1674-1137/42/12/123102. arXiv:1711.10289 [hep-ph].
- [12] Z. X. Zhao, Eur. Phys. J. C **78**, no. 9, 756 (2018), doi:10.1140/epjc/s10052-018-6213-2. [arXiv:1805.10878 [hep-ph]].
- [13] Z. P. Xing and Z. X. Zhao, Phys. Rev. D **98**, no. 5, 056002 (2018), doi:10.1103/PhysRevD.98.056002. [arXiv:1807.03101 [hep-ph]].
- [14] Y. M. Wang, Y. B. Wei, Y. L. Shen and C. D. Lü, JHEP **1706**, 062 (2017). doi:10.1007/JHEP06(2017)062[arXiv:1701.06810 [hep-ph]].
- [15] Y. M. Wang and Y. L. Shen, JHEP **1805**, 184 (2018). doi:10.1007/JHEP05(2018)184[arXiv:1803.06667 [hep-ph]].
- [16] Y. L. Shen, Y. B. Wei and C. D. Lü, Phys. Rev. D **97**, no. 5,054004 (2018). doi:10.1103/PhysRevD.97.054004[arXiv:1607.08727 [hep-ph]].
- [17] Y. Li and C. D. Lü, Sci. Bull. **63**, 267 (2018) doi:10.1016/j.scib.2018.02.003 [arXiv:1808.02990 [hep-ph]].
- [18] H. n. Li, C. D. Lu and F. S. Yu, Phys. Rev. D **86**, 036012 (2012). doi:10.1103/PhysRevD.86.036012 [arXiv:1203.3120 [hep-ph]].
- [19] F. S. Yu, H. Y. Jiang, R. H. Li, C. D. Lü, W. Wang and Z. X. Zhao, Chin. Phys. C **42**, no. 5, 051001 (2018) doi:10.1088/1674-1137/42/5/051001 [arXiv:1703.09086 [hep-ph]].

- [20] L. J. Jiang, B. He and R. H. Li, *Eur. Phys. J. C* **78**, no. 11, 961 (2018) doi:10.1140/epjc/s10052-018-6445-1 [arXiv:1810.00541 [hep-ph]].
- [21] R. Aaij *et al.* [LHCb Collaboration], arXiv:1905.02421 [hep-ex].
- [22] C. D. Lu, Y. M. Wang, H. Zou, A. Ali and G. Kramer, *Phys. Rev. D* **80**, 034011 (2009) doi:10.1103/PhysRevD.80.034011 [arXiv:0906.1479 [hep-ph]].
- [23] G. 't Hooft, *Nucl. Phys. B* **72**, 461 (1974). doi:10.1016/0550-3213(74)90154-0; A. J. Buras, J. M. Gerard and R. Ruckl, *Nucl. Phys. B* **268**, 16 (1986). doi:10.1016/0550-3213(86)90200-2.
- [24] CKMfitter Group (J. Charles *et al.*), *Eur. Phys. J. C* **41**, 1-131 (2005) [hep-ph/0406184], updated results and plots available at: <http://ckmfitter.in2p3.fr>
- [25] J. W. Li, M. Z. Yang and D. S. Du, *HEPNP* **27**, 665 (2003) [hep-ph/0206154]; M. Ablikim, D. S. Du and M. Z. Yang, *Phys. Lett. B* **536**, 34 (2002) doi:10.1016/S0370-2693(02)01812-9 [hep-ph/0201168]; X. Q. Li and B. S. Zou, *Phys. Lett. B* **399**, 297 (1997) doi:10.1016/S0370-2693(97)00308-0 [hep-ph/9611223]; Y. S. Dai, D. S. Du, X. Q. Li, Z. T. Wei and B. S. Zou, *Phys. Rev. D* **60**, 014014 (1999) doi:10.1103/PhysRevD.60.014014 [hep-ph/9903204]; M. P. Locher, Y. Lu and B. S. Zou, *Z. Phys. A* **347**, 281 (1994) doi:10.1007/BF01289796 [nucl-th/9311021].
- [26] X. H. Hu, R. H. Li and Z. P. Xing, *Eur. Phys. J. C* **80**, no.4, 320 (2020) doi:10.1140/epjc/s10052-020-7851-8 [arXiv:2001.06375 [hep-ph]].
- [27] A. Ali, G. Kramer, Y. Li, C. D. Lu, Y. L. Shen, W. Wang and Y. M. Wang, *Phys. Rev. D* **76**, 074018 (2007) doi:10.1103/PhysRevD.76.074018 [hep-ph/0703162 [HEP-PH]].
- [28] H. Y. Cheng, C. K. Chua and A. Soni, *Phys. Rev. D* **71**, 014030 (2005) doi:10.1103/PhysRevD.71.014030 [hep-ph/0409317].
- [29] C. D. Lu, Y. L. Shen and W. Wang, *Phys. Rev. D* **73**, 034005 (2006) doi:10.1103/PhysRevD.73.034005 [hep-ph/0511255]; G. Li and W. Wang, *Phys. Lett. B* **733**, 100 (2014) doi:10.1016/j.physletb.2014.04.029 [arXiv:1402.6463 [hep-ph]].
- [30] T. M. Yan, H. Y. Cheng, C. Y. Cheung, G. L. Lin, Y. C. Lin and H. L. Yu, *Phys. Rev. D* **46**, 1148 (1992) Erratum: [*Phys. Rev. D* **55**, 5851 (1997)]. doi:10.1103/PhysRevD.46.1148, 10.1103/PhysRevD.55.5851
- [31] R. Casalbuoni, A. Deandrea, N. Di Bartolomeo, R. Gatto, F. Feruglio and G. Nardulli, *Phys. Rept.* **281**, 145 (1997) doi:10.1016/S0370-1573(96)00027-0 [hep-ph/9605342].
- [32] U. G. Meissner, *Phys. Rept.* **161**, 213 (1988). doi:10.1016/0370-1573(88)90090-7
- [33] N. Li and S. L. Zhu, *Phys. Rev. D* **86**, 014020 (2012) doi:10.1103/PhysRevD.86.014020 [arXiv:1204.3364 [hep-ph]].
- [34] T. M. Aliev, A. Ozpineci, S. B. Yakovlev and V. Zamiralov, *Phys. Rev. D* **74**, 116001 (2006). doi:10.1103/PhysRevD.74.116001
- [35] T. M. Aliev, A. Ozpineci, M. Savci and V. S. Zamiralov, *Phys. Rev. D* **80**, 016010 (2009) doi:10.1103/PhysRevD.80.016010 [arXiv:0905.4664 [hep-ph]].
- [36] A. Khodjamirian, C. Klein, T. Mannel and Y.-M. Wang, *JHEP* **1109**, 106 (2011) doi:10.1007/JHEP09(2011)106 [arXiv:1108.2971 [hep-ph]].
- [37] K. Azizi, Y. Sarac and H. Sundu, *Phys. Rev. D* **90**, no. 11, 114011 (2014) doi:10.1103/PhysRevD.90.114011 [arXiv:1410.7548 [hep-ph]].
- [38] G. L. Yu, Z. G. Wang and Z. Y. Li, *Chin. Phys. C* **41**, no. 8, 083104 (2017) doi:10.1088/1674-1137/41/8/083104 [arXiv:1608.03460 [hep-ph]].
- [39] K. Azizi, Y. Sarac and H. Sundu, *Nucl. Phys. A* **943**, 159 (2015) doi:10.1016/j.nuclphysa.2015.09.005 [arXiv:1501.05084 [hep-ph]].
- [40] A. Ballon-Bayona, G. Krein and C. Miller, *Phys. Rev. D* **96**, no. 1, 014017 (2017) doi:10.1103/PhysRevD.96.014017 [arXiv:1702.08417 [hep-ph]].
- [41] T. Feldmann, P. Kroll and B. Stech, *Phys. Rev. D* **58**, 114006 (1998) doi:10.1103/PhysRevD.58.114006 [hep-ph/9802409].
- [42] H. M. Choi, C. R. Ji, Z. Li and H. Y. Ryu, *Phys. Rev. C* **92**, no. 5, 055203 (2015) doi:10.1103/PhysRevC.92.055203 [arXiv:1502.03078 [hep-ph]].
- [43] M. Tanabashi *et al.* (Particle Data Group), *Phys. Rev. D* **98**, 030001 (2018).
- [44] H. Y. Cheng and Y. L. Shi, *Phys. Rev. D* **98**, no.11, 113005 (2018) doi:10.1103/PhysRevD.98.113005 [arXiv:1809.08102 [hep-ph]].